

Offline World Models as Imagination Networks in Cognitive Agents

Saurabh Ranjan and Brian Odegaard

Department of Psychology, University of Florida

Author Note

ORCID:

Saurabh Ranjan: <https://orcid.org/0000-0002-7868-7223>

Brian Odegaard: <https://orcid.org/0000-0002-5459-1884>

Address Correspondence to:

Saurabh Ranjan: ranjan.saurabh@outlook.com

Brian Odegaard: bodegaard@ufl.edu

Competing interests: No competing interests to declare.

Author Contributions:

S.R.: Conceptualization, Visualization, Software, Methodology, Formal analysis, Data curation, Writing – original draft, Writing – review & editing.

B.O.: Writing – review & editing, Supervision.

Funding: S.R. was supported by the Threadgill Dissertation Fellowship from the University of Florida for this work.

Code and Data Availability: Code is available on github (https://github.com/saurabhr/imagine_world_model).

Complied data on OSF (<https://osf.io/658kw>). Additionally used open source datasets used for VVIQ-2 is available here:

<https://osf.io/vh4es/> and for PSIQ here: <https://datadryad.org/dataset/doi:10.5061/dryad.2v6wwpzt3>.

Abstract

The computational role of imagination remains debated. While classical accounts emphasize reward maximization, emerging evidence suggests it accesses internal world models (IWMs). We employ psychological network analysis to compare IWMs in humans and large language models (LLMs) via imagination vividness ratings, distinguishing offline world models (persistent memory structures accessed independent of immediate goals) from online models (task-specific representations). Analyzing 2,743 humans across three populations and six LLM variants, we find human imagination networks exhibit robust structural consistency, with high centrality correlations and aligned clustering. LLMs show minimal clustering and weak correlations with human networks, even with conversational memory, across environmental and sensory contexts. These differences highlight disparities in how biological and artificial systems organize internal representations. Our framework offers quantitative metrics for evaluating offline world models in cognitive agents.

Keywords: imagination, world model, vividness, network science, artificial intelligence

Offline World Models as Imagination Networks in Cognitive Agents

Understanding how cognitive systems internally represent the world is central to both cognitive science and artificial intelligence¹⁻³. Imagination occurs without external input, and provides a window into these internal models through its role in planning⁴, reasoning⁵, and learning⁶. Classical reinforcement learning frameworks propose that imagination optimizes reward prediction⁶⁻⁹ yet accumulating evidence challenges this view^{10,11}. Humans can imagine without explicit rewards during creativity, daydreaming, and aesthetic contemplation¹²⁻¹⁴. This suggests a broader computational role: imagination accesses structured internal world models that persist independent of immediate task demands.

Previous attempts to characterize internal world models in Large Language Models (LLMs) have yielded mixed findings, and definitions of world models have been contingent upon specific task characteristics. For example, some researchers have utilized the map of Manhattan as the base world model to train AI models to navigate between locations within it¹⁵. Their findings revealed that AI models do not show an implicit map of the world, and that the map could not be recovered from their responses. On the other hand, it has also been demonstrated that LLM-like models exhibit emergent properties, demonstrating their knowledge for unobserved and intermediate stages of a grid world¹⁶. However, both of these examples lack comparison with human behavior.

Much of the knowledge about internal world models in both humans and LLMs comes from understanding how predictive or hypothetical actions are encoded with task-related states¹⁷⁻¹⁹. World models in existing work are characterized through goal-directed tasks^{17,18,20,21} with explicit rewards or performance optimization for navigation¹⁵ and prediction of hidden states²². In contrast, our approach of having agents imagine scenes and providing vividness

constitutes non-goal-directed behavior where there is no active goal pursuit in a trial for reward¹⁷; participants simply report transparently the vividness of their experience, accessing memory representations using their imagination rather than building task-specific *world models* in goal pursuit. Building on these findings, we propose a fundamental distinction for world models: online world models constitute task-specific representations mapping actions to outcomes during goal pursuit^{23,24}. In contrast, offline world models comprise background knowledge structures that organize experience independent of current tasks. This distinction addresses a computational puzzle: humans spend substantial time in non-goal-directed mental states¹²⁻¹⁴ where internal representations remain rich and structured despite absent task demands. Current frameworks emphasizing action-reward mappings provide incomplete accounts of these offline states^{17,23,24}, which may fundamentally constrain online task performance. Humans rating imagination vividness requires accessing pre-existing phenomenological knowledge without learning rewards for an ongoing task, prediction, or optimization across trials. While participants do follow task instructions, they are not constructing new action-outcome mappings or reward predictions; they simply report standing knowledge about how scenarios are subjectively experienced. This distinction isolates background knowledge structures from the active, goal-directed processes that construct task-specific models.

Relatedly, in artificial intelligence research, it has been proposed that imagination's role is to access the "world model" that a deep-learning model would have learned from the training data²⁵. But to date, it remains unclear what the representational properties of such an internal offline world model actually are, and whether humans and AI models have similar representational characteristics. Recently proposed *hierarchical* and *heterarchical models of imagination*²⁶⁻²⁸ posit that imagination involves semantic memory, episodic memory, attention,

and working memory, utilizing domain-preferring brain areas that are bridged *heterarchically* by the domain-general fusiform imagery node (FIN) and *hierarchically* by parietal regions. Recent theoretical work in cognitive neuroscience posits that these heterarchical systems that model reality may be needed to truly understand language and the world itself²⁸. This work implies that when we imagine heterogenous contents, they still can be related to each other due to the shared neural processes involved during their experience.

Based on emerging ideas in cognitive neuroscience, we hypothesize that patterns of vividness ratings across imagined scenarios provide quantifiable signatures of offline world model organization. Vividness is the subjective intensity of mental imagery, which represents a stable individual trait²⁹ measurable through validated instruments including the Vividness of Visual Imagery Questionnaire (VVIQ-2)³⁰ and Plymouth Sensory Imagery Questionnaire (PSIQ)³¹. These text-based assessments enable direct comparison between humans and large language models (LLMs). Emerging evidence with LLM's suggests that even minimal sensory-style instructions (e.g., “imagine seeing...”) can guide text-only LLMs to organize their internal representations in ways that parallel modality-specific encoders³². Thus, prompting may be sufficient to evoke structured, perceptual-like processing³². If imagination accesses and samples from an offline world model, dependencies among vividness ratings should reveal underlying structural organization. Critically, our text-based imagery assessments enable direct comparison of offline world models between humans and large language models (LLMs), which we treat as cognitive agents whose parameters encode world knowledge through training^{33,34}.

Here, we introduce imagination networks: graph-theoretic representations where nodes denote imagined scenarios and edges capture vividness rating associations. Network science provides principled metrics for quantifying organizational structure³⁵. We employ network

centrality metrics to quantify node importance through different mechanisms, as expected influence and strength measure direct connections, while closeness and betweenness capture global information flow^{36–38}. Further, we implement community detection algorithms to identify clustering patterns reflecting organizational principles^{39–41}. We test whether offline world models showed similar structures across human populations, and whether current LLMs replicate these organizational features. Specifically, we show correlated centrality values and aligned clustering across populations. Given that human offline world models emerge from multimodal, embodied experience while LLM representations derive from linguistic statistics, we predict systematic structural differences in their imagination networks.

Results

Human and LLM populations show distinct vividness distributions

We used vividness ratings from human participants across two validated imagination questionnaires: the VVIQ-2 (32 items spanning 8 environmental scene contexts with a 1 to 5 point scale) from Florida (N = 541) and Poland (N = 1,651), and the PSIQ (21 items across 7 sensory modalities with a 0 to 10 point scale) from Florida (N = 334), London (N = 217), and Florida+London (N = 551). For the VVIQ-2, we randomly subsampled 2 non-overlapping groups of N = 600 from the Poland group (N = 1,651) to compare the total vividness, centrality and clustering within groups as well as across groups with Florida (N = 541) and Florida+Poland (N = 2192). The Florida and London groups performed PSIQ and VVIQ-2 in English and the Polish group performed the VVIQ-2 in the Polish language. To enable comparison with humans, we generated LLM responses using six model variants: Gemma3-12B, Gemma3-27B, their quantization-aware trained counterparts (Gemma3-12B-QAT, Gemma3-27B-QAT), Llama3.3-70B, and Llama4x16x17B (mixture-of-experts architecture) by

matching the total vividness distribution with the human groups (*See Methods*). Each model produced 1,000 simulations by crossing 200 synthetic personas⁴² with five imagination ability conditions: *aphantasia* (no imagery), *hypophantasia* (reduced imagery), *typical imagery*, *hyperphantasia* (extremely vivid imagery), and *no explicit instruction* and their effects can be observed in the *Fig 1A*. We tested two conversational conditions: independent (stateless, with each item rated without any memory of previous responses) and cumulative (with conversational memory maintained across sequential items).

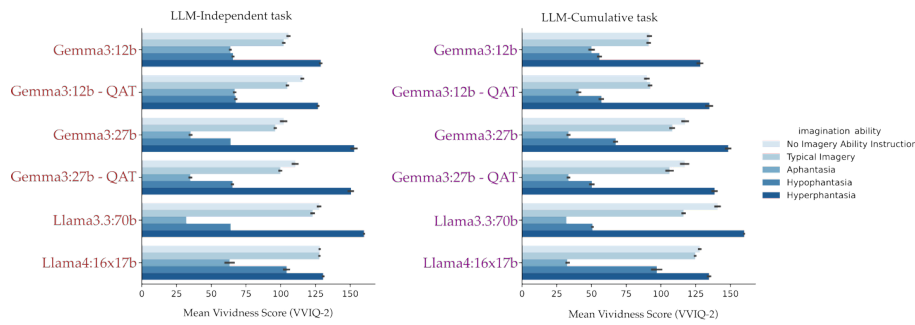
Total vividness scores are the sum of scores across all the questionnaire items, which revealed systematic differences on LLMs with the imagination condition ability prompt. For the VVIQ-2 (theoretical range 32-160), Kruskal-Wallis tests demonstrated significant main effects of imagination ability instruction ($H(4)=9,588$, $p<10^{-7}$), conversational condition ($H(1)=49.2$, $p=2\times 10^{-12}$), and model architecture ($H(5)=461$, $p<10^{-97}$) as shown in *Fig. 1A*. Dunn's post-hoc tests revealed that scores increased monotonically with prompted imagination ability, from aphantasia instructions (mean=43.2, 95% CI [42.8, 43.6]) to hyperphantasia (mean=141.3, 95%CI [140.7, 141.9]). Unexpectedly, the no-instruction condition produced higher scores (mean=114.6, 95%CI [114.0, 115.2]) than explicit typical imagery prompts (mean=107.8 [107.2, 108.4]), suggesting LLMs default to vivid imagination absent explicit constraints. The cumulative conversational condition increased total scores by 5.4% relative to independent (97.4 vs 92.3), and scores scaled systematically with model size (Gemma3-12B: 88.3, 95%CI [87.7, 88.9]; Llama4-16x17B: 107.1, 95%CI [106.4, 107.8]). Similar patterns emerged for the PSIQ (*Fig. S1A*).

To construct LLM populations matching human imagination ability diversity, we downsampled each model's 1,000 simulations to 600 based on human total vividness score

distributions (Methods). Kolmogorov-Smirnov tests revealed that all LLM distributions differed significantly from all human populations (all $D > 0.15$, $p < 0.001$ after FDR correction; Fig. 1B). Within humans, most populations showed statistically similar distributions (exceptions included Florida vs Florida+Poland $D = 0.07$, $p_{BH} = 0.035$; Poland-1 vs Poland-All $D = 0.11$, $p_{BH} < 0.001$), confirming that human imagination ability profiles are conserved across geographic populations (total vividness scores and their distribution are displayed in *Fig. 1B*).

These univariate analyses establish that LLMs can produce controllable vividness responses sensitive to prompting manipulations. However, total vividness scores, being simple sums across items, provide no insight into how imagined scenarios relate to one another within a cognitive agent's internal representations. A person or model could achieve identical total scores through entirely different patterns of scenario-specific vividness, reflecting fundamentally different organizational structures. To characterize the relational architecture of offline world models, we therefore turned to multivariate network analysis, which captures how vividness patterns across scenarios reveal the underlying representational organization that univariate statistics cannot detect.

A. LLM’s mean vividness across imagination ability.



B. Mean (left) and distribution (right) of total vividness score in Humans and after population diversity sampling in LLMs.

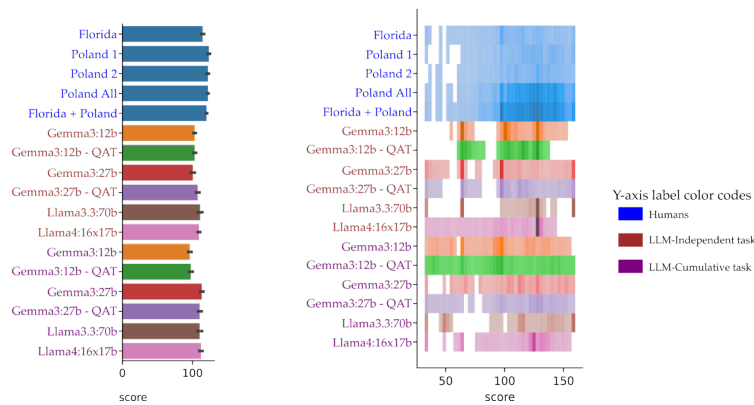


Fig 1. Total VVIQ-2 vividness scores and distributions in LLMs and human populations. (A) Mean vividness scores across different VVIQ-2 LLM simulations. The total score is the sum of all vividness ratings in the questionnaire in independent item sampling (left) and conversational memory sampling (right). For each LLM in a task (independent or cumulative) with total 1000 simulations generated using 200 personalities and five imagination ability conditions. (B) (*Left*) Average total vividness scores from human populations in (blue) Florida ($N = 541$), Poland-1 ($N = 600$), Poland-2 ($N = 600$), Poland-All ($N = 1651$), Florida+Poland ($N = 2192$). Each LLM agent after population diversity sampling (to match variability in the imagination abilities of LLMs with humans; see Methods), with 600 simulations from different imagination abilities. (*Right*) Distributions of the total vividness scores in humans and LLM agents for the VVIQ-2. Darker colors denote a higher density of data in that bin for a given population of cognitive agents (human or LLM). See Fig. S1 for vividness scores for the PSIQ. The error bars in bar plots are bootstrapped ($N = 1000$) 95% confidence intervals.

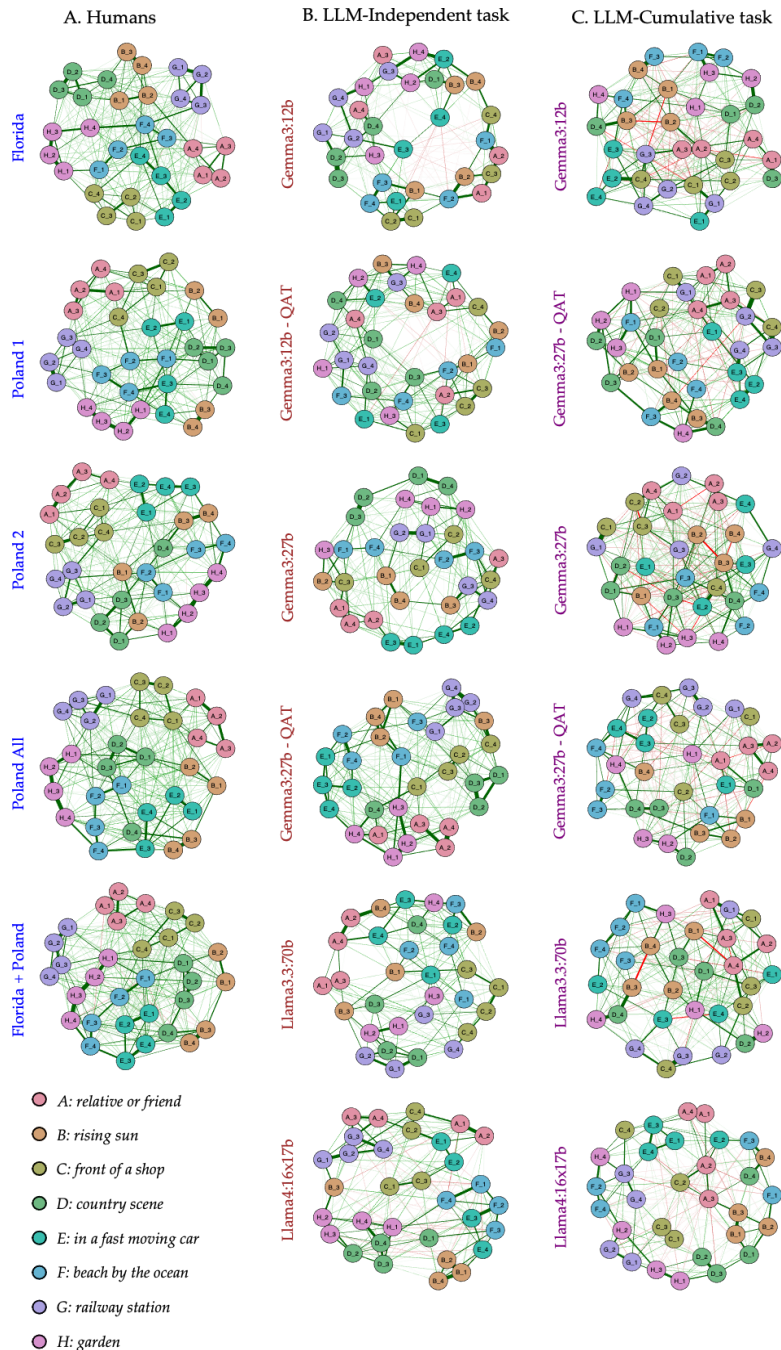


Fig. 2. Imagination networks using the VVIQ-2 in Humans and LLMs. Cognitive agents (humans or LLMs) report the vividness of imagined items across different contexts of the environment, denoted as different colors in the networks. There are four items in each context, with postfixed numerals labeling each node. The vividness rating is reported on a scale of 1 to 5. The network was estimated using the EbicGlasso method using Spearman partial correlations of vividness ratings between different pairs of nodes. (A) Imagination networks in human populations: Florida ($N = 541$), Poland-1 ($N = 600$), Poland-2 ($N = 600$), Poland-All ($N = 1651$), Florida+Poland ($N = 2192$), from top to bottom. (B) LLM imagination networks from Gemma and Llama variants in independent task conditions. (C) In the LLM imagination networks in the cumulative task condition, each scene’s vividness rating is provided utilizing the conversation history of previous interactions (i.e., previous responses to items on the questionnaire). Each LLM network consists of $N = 600$ simulations. The color of nodes signifies the context in the VVIQ-2 with four items in each context. The color and thickness of an edge indicates its magnitude and direction of association. Red lines indicate negative associations and green lines indicate positive associations for an edge.

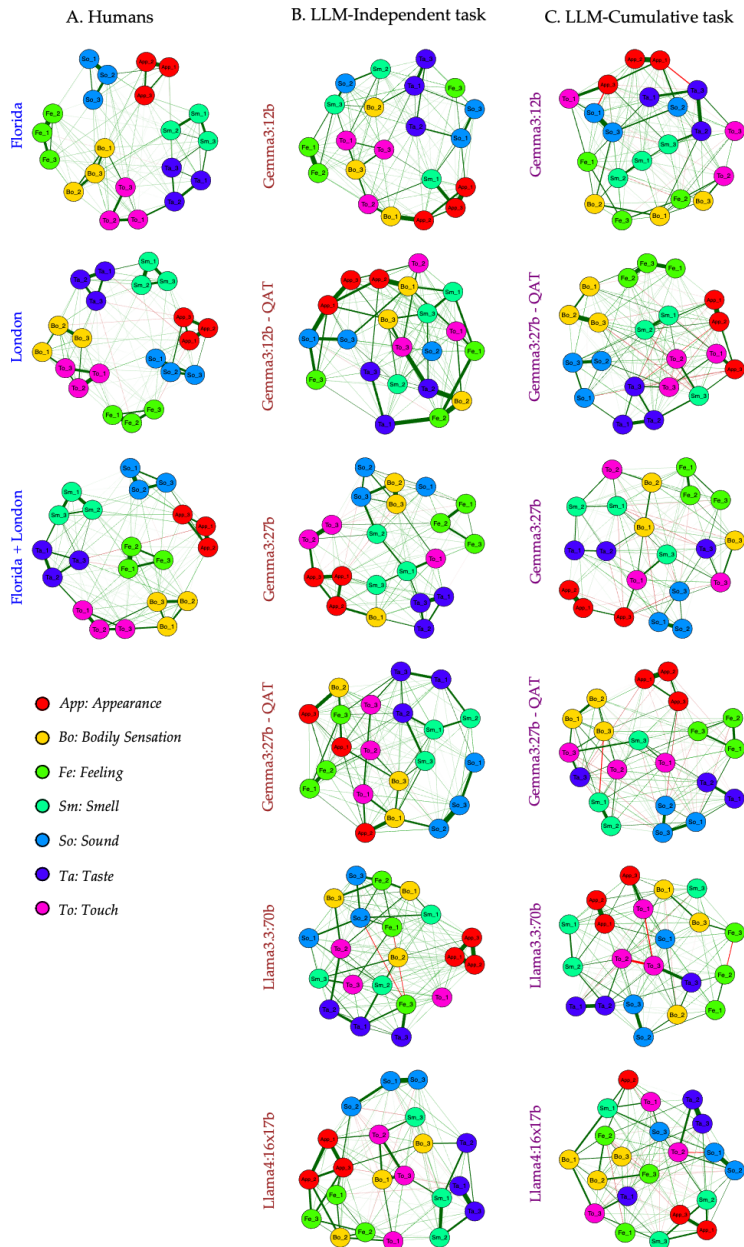


Fig. 3. Imagination networks using the PSIQ in Humans and LLMs. Cognitive agents (humans or LLMs) report the vividness of imagined items across different contexts of sensory experiences, denoted as different colors in the networks. There are three items in each context, with postfixed numerals to each node. The vividness rating is reported on a scale of 0 to 10. The network is estimated using the EbicGlasso method using Spearman partial correlations of vividness ratings between different pairs of nodes. (A) Imagination networks in human populations: Florida ($N = 334$), London ($N = 217$), and Florida+London ($N = 551$), from top to bottom. (B) LLM imagination networks in the independent task condition. Each node's vividness rating is rated independently. (C) In the LLM imagination networks in the cumulative task condition, each item's vividness rating is rated with the conversation history of previous interactions. Each LLM network consists of $N = 600$ simulations. The color of nodes signifies the modality in the PSIQ, with three items in each modality. The color and thickness of an edge indicate its magnitude and direction of association. Red lines indicate negative associations and green lines indicate positive associations for an edge.

Expected influence and strength reveal high correlations within human populations, highlighting the importance of nodes in imagination networks

We constructed imagination networks from vividness rating matrices using regularized partial correlations (EBICglasso method with Spearman correlations^{40,43}; Figs. 2, 3). Local centrality measures included expected influence and strength, which quantify node importance through direct network connections; these measures revealed striking structural consistency across human populations.

For the VVIQ-2 expected influence centrality, within-Poland population centrality correlations were strong: Poland-1 vs Poland-2 ($r=0.712$, 95% CI [0.525, 0.833], $p<10^{-5}$), Poland-1 vs Poland-All ($r=0.931$ [0.882, 0.961], $p<10^{-15}$), and Poland-2 vs Poland-All ($r=0.860$, $p<10^{-10}$). Cross-population comparisons between Florida and Poland groups showed moderate to strong correlations: Florida vs Poland-1 ($r=0.589$ [0.347, 0.754], $p=2\times 10^{-4}$, $p_{BH}=0.002$), Florida vs Poland-2 ($r=0.466$, $p=0.0036$, $p_{BH}=0.030$), and Florida vs Poland-All ($r=0.595$, $p=1.6\times 10^{-4}$, $p_{BH}=0.002$). Critically, composite populations containing overlapping participants showed enhanced correlations compared to constituent groups: Florida vs Florida+Poland ($r=0.732$ [0.554, 0.845], $p<10^{-6}$), Poland-1 vs Florida+Poland ($r=0.920$, $p<10^{-15}$), and Poland-All vs Florida+Poland ($r=0.999$, $p<10^{-30}$; Fig. 4A-1). Similar patterns emerged for the human populations' PSIQ imagination networks: Florida vs London ($r=0.425$, $p=0.027$), Florida vs Florida+London ($r=0.914$ [0.810, 0.963], $p<10^{-9}$), and London vs Florida+London ($r=0.733$, $p=7.9\times 10^{-5}$; Fig. 4B-1).

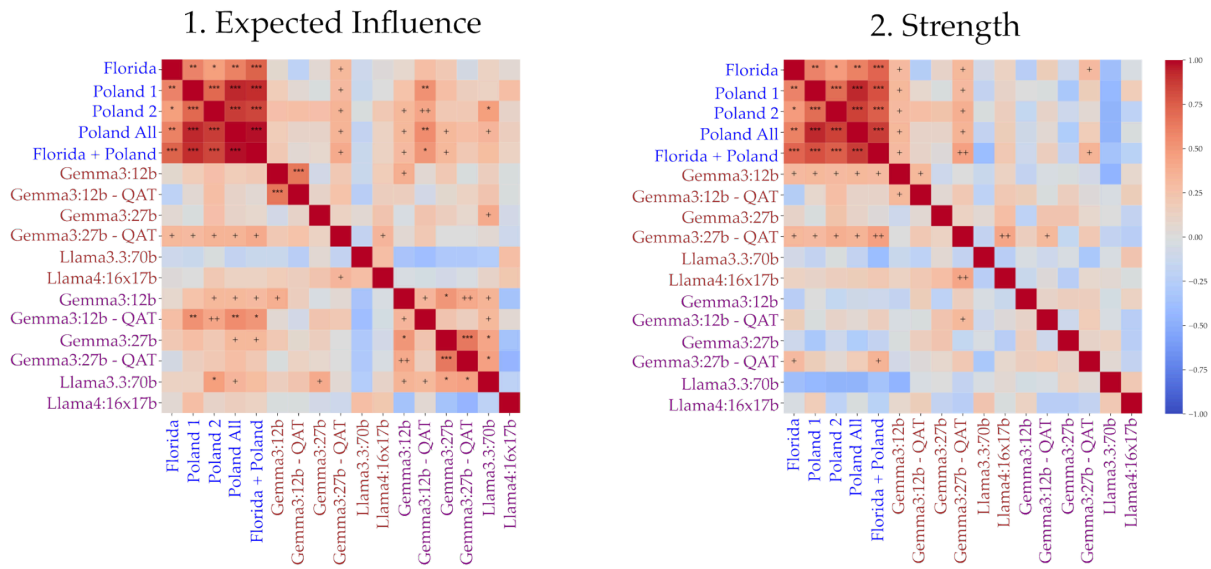
Strength centrality, the sum of unsigned edge weights, showed similar results across human populations. For the VVIQ-2: Florida vs Poland-1 ($r=0.591$, $p=1.8\times 10^{-4}$, $p_{BH}=0.003$), Poland-1 vs Poland-2 ($r=0.692$, $p<10^{-5}$), Poland-1 vs Poland-All ($r=0.928$, $p<10^{-15}$), and Florida

vs Florida+Poland ($r=0.725$, $p<10^{-6}$; Fig. 4A-2). For PSIQ: Florida vs Florida+London ($r=0.858$, $p<10^{-6}$), and London vs Florida+London ($r=0.538$, $p=0.006$; Fig. 4B-2).

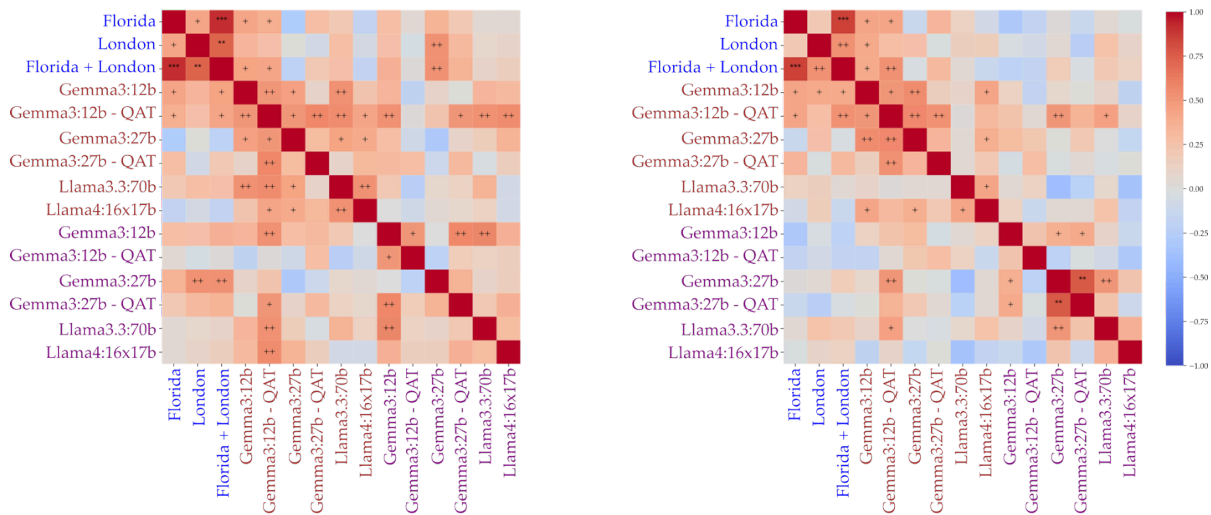
In stark contrast, LLM networks showed weak and inconsistent correlations with human networks. Of the possible LLM-human pairwise comparisons for VVIQ-2 expected influence, only 8 achieved significance after FDR correction: Gemma3-27B-QAT in the independent condition showed weak correlations with human populations ($r=0.308-0.393$, $p_{BH}=0.04-0.08$), while four models in the cumulative condition showed modest improvements (Gemma3-12B, Gemma3-12B-QAT, Gemma3-27B, Llama3.3-70B; maximum $r=0.548$ for Gemma3-12B-QAT vs Poland-All, $p_{BH}=0.007$). The PSIQ showed only 6 of 72 possible comparisons reaching significance. Median LLM-human expected influence correlation was $r=0.13$ for VVIQ-2 and $r=0.09$ for PSIQ, compared to median human-human correlations of $r=0.66$ (VVIQ-2) and $r=0.76$ (PSIQ), representing an approximately 5-fold difference in structural alignment.

For strength centrality in the VVIQ-2, only Gemma3-12B and Gemma3-27B-QAT showed significant correlations in independent condition ($r=0.302-0.452$ across human populations), while the cumulative condition yielded sporadic significance that rarely survived multiple comparison correction. PSIQ strength showed similar patterns: Gemma3-12B correlated with all human groups in independent mode ($r=0.404-0.422$), but most other configurations showed null results. Overall, local centrality measures demonstrate that human populations share highly conserved network organizational principles that current LLMs fail to replicate.

A. VVIQ-2 Local Centrality Correlations



B. PSIQ Local Centrality Correlations



Label color codes ■ Humans ■ LLM-Independent task ■ LLM-Cumulative task

Fig. 4. Pearson’s r correlation heatmaps of node importance using different local centrality measures across VVIQ-2 and PSIQ imagination networks. The left column denotes correlations for expected influence; the right column denotes correlations for strength. (A) Centrality correlations among cognitive agents for the nodes in VVIQ-2 imagination networks with 32 nodes (*top row*). (B) Centrality correlations among cognitive agents for the nodes in PSIQ imagination networks with 21 nodes (*bottom row*). Expected influence and strength centralities exhibited high correlations among human populations for the VVIQ-2, and a similar pattern of results was found for the PSIQ. + denotes a significant result based on uncorrected p-values and * denotes significant result based on corrected p-values using Benjamini/Hochberg FDR correction for multiple comparisons; */+ < 0.05; **/+ < 0.01; *** < 0.001. The heatmaps are symmetric across the top-left to bottom-right diagonal.

In humans, imagined nodes are highly correlated for closeness, but not for betweenness centrality

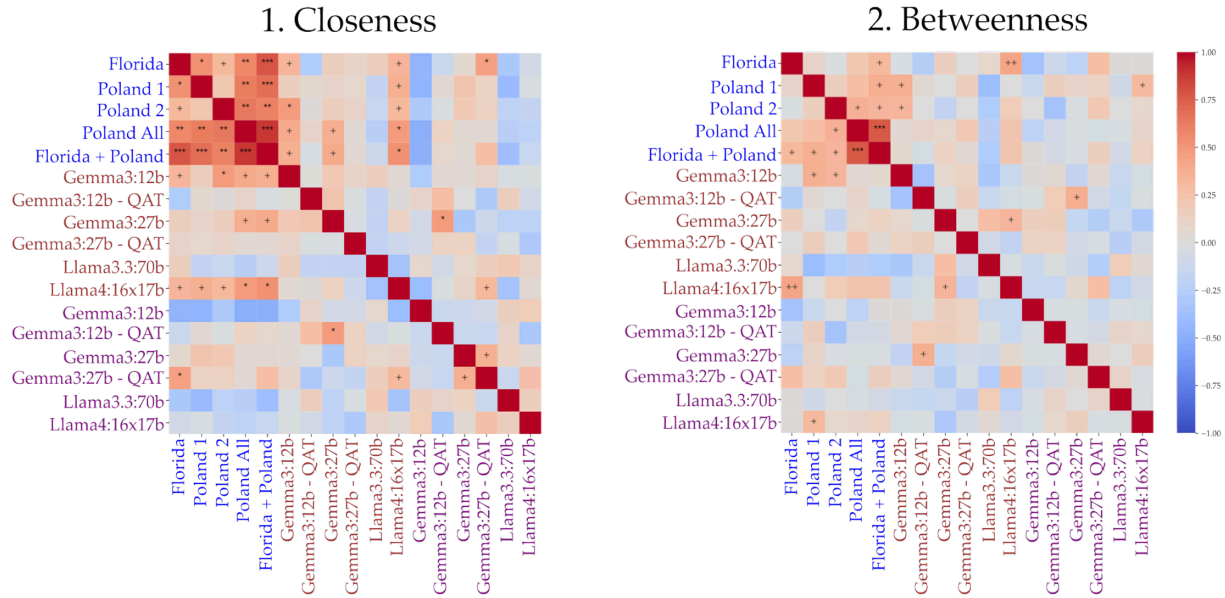
Closeness centrality is the measurement of how efficiently information flows from a node to all other nodes via the shortest network paths; this measure revealed robust correlations across human imagination networks. For the VVIQ-2, all human population pairs showed significant positive correlations: Florida vs Poland-1 ($r=0.535$, $p=7.9\times 10^{-4}$, $p_{BH}=0.014$), Florida vs Poland-2 ($r=0.313$, $p=0.041$), Florida vs Poland-All ($r=0.572$, $p=3.1\times 10^{-4}$, $p_{BH}=0.006$), Florida vs Florida+Poland ($r=0.776$, $p<10^{-6}$), Poland-1 vs Poland-All ($r=0.619$, $p=8.0\times 10^{-5}$, $p_{BH}=0.002$), Poland-2 vs Poland-All ($r=0.640$, $p=4.0\times 10^{-5}$, $p_{BH}=0.001$), and Poland-All vs Florida+Poland ($r=0.884$, $p<10^{-10}$; Fig. 5A-1). PSIQ networks exhibited even stronger closeness correlations: Florida vs London ($r=0.759$, $p=3.3\times 10^{-5}$, $p_{BH}=0.001$), Florida vs Florida+London ($r=0.874$, $p<10^{-7}$), and London vs Florida+London ($r=0.842$, $p<10^{-6}$; Fig. 5B-1).

LLM networks showed inconsistent closeness correlations with humans, though with notably better performance than local centrality measures. For the VVIQ-2, correlations remained sparse (9 of 144 comparisons significant), but the PSIQ showed modest improvement (15 of 72 comparisons significant), suggesting LLMs may better approximate sensory concept organization than environmental scene structure. This task-dependent asymmetry implies differential alignment with specific aspects of human world models.

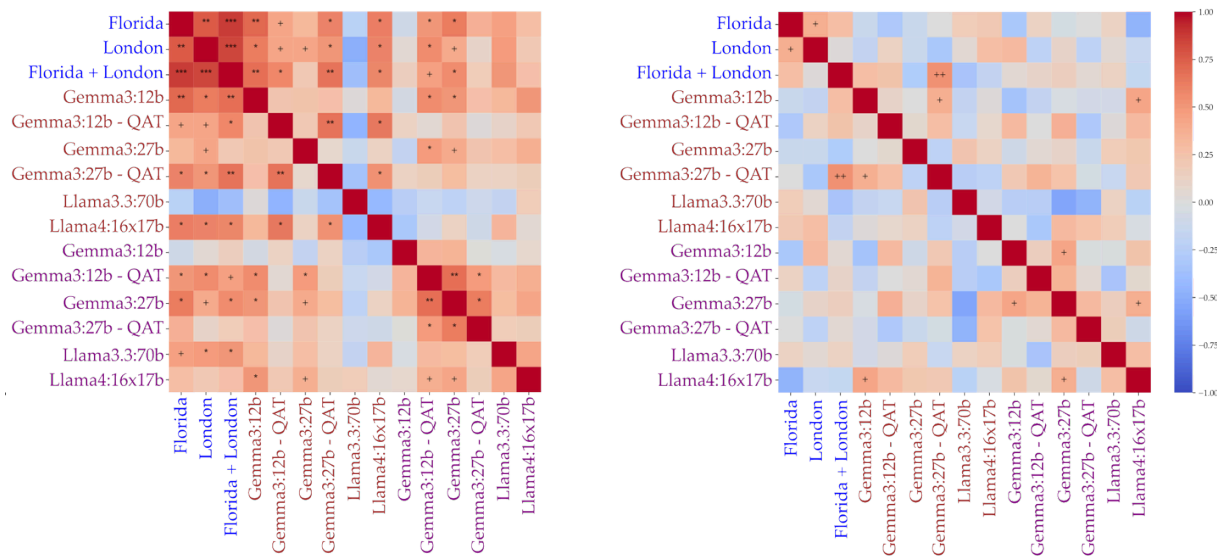
Betweenness centrality quantifies how frequently a node appears in shortest paths between other node pairs; this measure showed universally weak correlations across all cognitive agent comparisons (median $r=0.08$ for all pairwise comparisons; Fig. 5A-2, 5B-2). Furthermore, betweenness demonstrated poor stability in case-dropping bootstrap analysis (CS-coefficient <0.25 for most networks; Tables S1-S2), indicating high sampling variability. The

weak correlations and low stability suggest that betweenness captures individual differences in how scenarios bridge different regions of imagination networks, likely reflecting personalized experiential histories that vary substantially even within populations sharing similar overall network structure.

A. VVIQ-2 Global Centrality Correlations



B. PSIQ Global Centrality Correlations



Label color codes ■ Humans ■ LLM-Independent task ■ LLM-Cumulative task

Fig. 5. Pearson’s r correlation heatmaps of node importance using different global centrality measures across VVIQ-2 and PSIQ imagination networks. Columns, left to right, display different centrality measures; specifically, closeness and betweenness. (A) Centrality correlations among cognitive agents for the nodes in VVIQ-2 imagination networks with 32 nodes (*top row*). (B) Centrality correlations among humans but not in betweenness for the nodes in PSIQ imagination networks with 21 nodes (*bottom row*). Closeness centrality correlations across cognitive agents show high correlations among human populations across VVIQ-2 and PSIQ. Betweenness centrality results show a lack of centrality correlations across cognitive agents in both VVIQ-2 and PSIQ. + denotes significance based on uncorrected p-values and * denotes significance based on corrected p-values using Benjamini/Hochberg FDR correction for multiple comparisons; */+ < 0.05; **/++ < 0.01; *** < 0.001. The heatmaps are symmetric across the top-left to bottom-right diagonal.

Clustering is prominent in human networks, and often absent in LLM agents for imagination networks.

Data-based clusters were computed from the imagination networks (Fig. 2 and Fig. 3) and calculated using the walk-trap algorithm⁴⁴ to measure the meso-level properties of the imagination networks. As centralities capture the micro-level properties of the network at the node level, one can investigate the meso-level characteristics of the network in terms of how a group of nodes cluster together^{37,45}. The walk-trap algorithm is a community detection algorithm that identifies communities/clusters of nodes characterized by dense connections among themselves, rather than to other nodes in the network. Community detection (walk-trap algorithm) revealed qualitative differences in network organization. Human VVIQ-2 networks decomposed into 4-6 modules reflecting questionnaire structure (Table S3), while 5 of 6 LLM models in independent conditions produced single-cluster networks. Cumulative memory increased clustering for some models (Gemma3-27B-QAT: 5 clusters), but patterns remained model-dependent. The PSIQ showed sharper contrasts: human networks yielded 4-5 clusters versus predominantly single-cluster LLM networks, except Gemma3-27B-QAT in cumulative mode (5 clusters; Table S4).

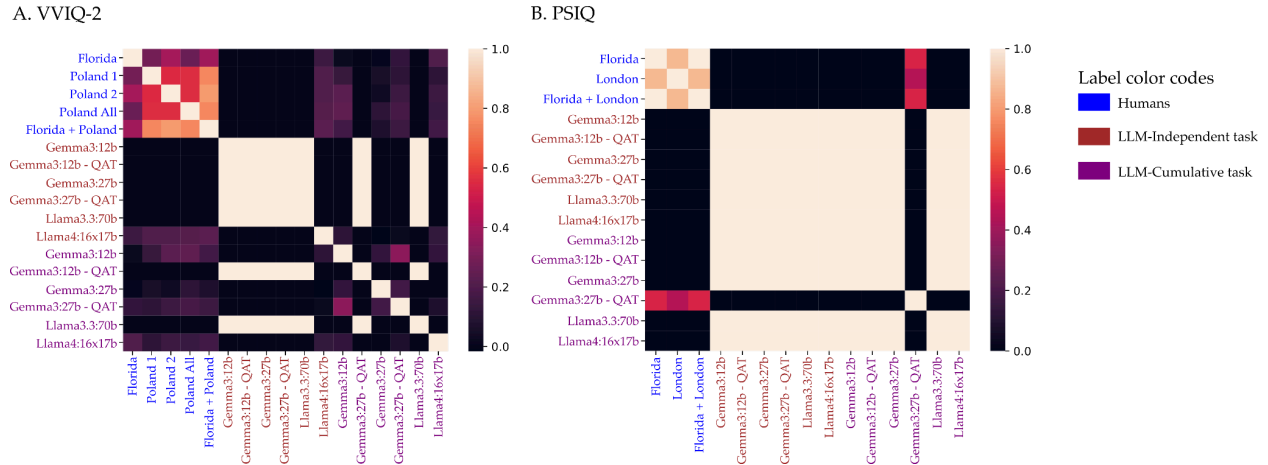


Fig. 6. Alignment of clusters across imagination networks, as measured using the Adjusted Rand Index. (A) Clustering alignment in the imagination network from the VVIQ-2 task. (B) Clustering alignment in the imagination network from the PSIQ task. The heatmap matrices are symmetric, from the top-left to the bottom-right diagonal.

In Fig. 6, the adjusted Rand Index (ARI) quantified clustering similarity (1.0=perfect alignment, 0=chance, negative=worse than chance). Human VVIQ-2 networks showed moderate alignment (ARI=0.27-0.40), while PSIQ networks exhibited strong alignment (ARI=0.87-1.0; Fig. 6). Most LLM independent-task networks achieved ARI=0 with humans due to degenerate single-cluster topology. The highest-performing model (Llama4-16x17B independent) reached ARI=0.22 (VVIQ-2). Cumulative memory improved some models (Gemma3-27B: ARI=0.30 for VVIQ-2; Gemma3-27B-QAT: ARI=0.54 for PSIQ), yet all remained below human-human alignment.

Discussion

Network analysis of imagination vividness ratings reveals systematic organizational differences between human and LLM offline world models. Human imagination networks demonstrate three key signatures of conserved structure: (i) correlated node importance across populations (expected influence $r=0.43-0.93$, closeness $r=0.31-0.88$), (ii) consistent multi-cluster organization (4-6 modules for VVIQ-2, 4-5 for PSIQ), and (iii) high inter-population clustering alignment in human populations. Measurements systematically increased when comparing

subpopulations to their parent populations, confirming structural consistency rather than sampling artifacts. Current LLMs fail to replicate these features, showing weak centrality correlations, predominantly degenerate single-cluster topologies, and minimal alignment with human networks (median ARI=0). These disparities persist across model architectures, scales (12B-70B parameters), task conditions, and imagination contexts.

The human-LLM divergence likely reflects different representational foundations. Human offline world models emerge through embodied, multimodal experience consolidated via episodic memory systems^{26,27,46,47}. Our results depend on the vividness ratings for imagined scenes, which quantify the subjective quality of an imagined experience. Vividness ratings tap phenomenological qualities: subjective intensity and experiential specificity, which are grounded in the human embodied mind perceptually^{48,49} and linguistically⁵⁰. Network structure presented above reflects how scenarios relate within this phenomenologically-organized knowledge. LLMs trained on linguistic co-occurrence statistics and meaning derived from an attention based mechanism which possesses semantic knowledge about sensory concepts^{32,51-53} but lack the experiential substrate generating structured phenomenology. This interpretation aligns with recent demonstrations that LLMs show topological similarity to humans for abstract semantic relationships (color similarity⁵³) but our results show divergence on scenarios requiring phenomenological grounding^{54,55}.

Our framework addresses a critical gap in world model theory. Existing accounts focus on online world models that are task-specific action-reward mappings during goal pursuit^{16-19,23,24}. We demonstrate that offline world models formed of background knowledge structures that are independent of immediate tasks exhibit measurable organizational principles. This distinction proves computationally important: humans occupy non-goal-directed mental

states (mind-wandering, aesthetic contemplation) representing substantial cognitive activity¹²⁻¹⁴. These states engage structured representations despite absent task demands, suggesting offline organization constitutes foundational cognitive architecture. The offline/online distinction likely represents complementary computational levels, where background structure (offline) constrains and enables task-specific model construction (online). Understanding offline world models may predict online performance: representation richness likely determines how effectively agents construct task-relevant models.

The conserved human structure suggests imagination networks may capture shared “recovery maps” representations encoding environmental transition dynamics⁵⁶. Our scenarios involve common experiences (rising sun, familiar sounds, moving through space), potentially yielding similar approximations of environmental state transitions through similar human experience of our natural surroundings. Network centrality quantifies how these scenarios relate, with high cross-population correlations indicating universal organizational principles. However, betweenness instability indicates individual bridging differences, likely reflecting personalized experiential histories and is in line with similar findings on betweenness centrality for psychological network analysis^{37,43}.

Current LLM limitations reveal architectural requirements for human-like offline world models. Neither parameter scale (12B to 70B), architectural sophistication (mixture-of-experts), nor conversational memory sufficed. This suggests offline organization emerges from qualitatively different mechanisms than next-token prediction with attention. Candidate mechanisms for offline world model in humans could include: (i) episodic memory systems enabling flexible experience recombination^{28,29,46,47} that are generative and compositional⁵⁷, (ii) multimodal grounding linking concepts to sensory-motor experience^{58,59} (iii) developmental

structuring through embodied environmental interaction, or (iv) conscious experience generating phenomenological organization^{60–62}.

Based on our approach for estimating geometrical properties of offline world models, certain limitations qualify for considerations. Ceiling effects in vividness (hyperrealistic imagination) would preclude network analysis and might indicate reality monitoring deficits as the imagination accesses the internal world model as vivid as the external world^{63,64}. Our static networks capture structure but not dynamics of active mental simulation^{11,65}, although the imagined scenarios could be dynamic (an example from the VVIQ-2 is “*Think of being driven in a fast-moving car by a relative or friend along a major highway.*” and similarly in PSIQ is “*Imagine the appearance of a cat climbing a tree.*”) in our investigations. Critical future directions include: (i) examining how imagination networks evolve dynamically, (ii) testing whether offline structure predicts online task performance, potentially explaining why AI systems succeed or fail at reasoning requiring human world knowledge, and (iii) investigating developmental trajectories of imagination network formation.

The PSIQ versus VVIQ-2 performance asymmetry (improved LLM closeness correlations) suggests task-dependent similarity as well as aligns with past findings on LLMs able to capture sensory information and its relation with each other^{32,51–53}. LLMs may better approximate explicit sensory concept organization than implicit episodic scene structure, potentially reflecting training corpus biases toward sensory descriptions over experiential narratives. This dissociation suggests imagination networks can diagnose specific representational gaps, enabling targeted architectural improvements for LLMs.

Our imagination network framework provides quantitative tools for comparing offline world models across cognitive agents. The systematic human-LLM differences are absent in

semantic similarity tasks^{32,51,53} suggest fundamental representational disparities in phenomenologically-grounded knowledge organization. These findings establish benchmarks for evaluating whether future AI systems achieve human-like offline world models, a potentially critical prerequisite for robust reasoning and flexible intelligence. By distinguishing offline from online world models, we highlight an underexplored dimension of cognitive architecture with implications for understanding both biological and artificial intelligence.

Methods

Participants

There were 541 participants (394 females and 147 males) in the VVIQ-2 Florida data, with a mean age of 20.4 years. The Florida dataset for both the VVIQ-2 and PSIQ was curated from responses provided by participants at the University of Florida, who received course credit for completing the task successfully. The data was collected from participants who gave consent prior to the start of the study. The study was approved by the Institutional Review Board of the University of Florida (IRB No.: ET00045024). For the Polish VVIQ-2 data, 1651 participants (1043 females and 608 males) fully completed the questionnaire from Jankowska & Karwowski (2022)⁶⁶, which comprises individuals from schools in Poland at the undergraduate level of college available here: <https://osf.io/vh4es/>. We created two non-overlapping subsets of 600 participants by randomly sampling the Polish dataset as “*Polish 1*” and “*Polish 2*,” whereas “*Polish All*” consists of all the data (1651 participants) from Poland in the results. We also analyzed the data by pooling all the data from the “Florida + Poland” group, which consisted of 2192 individuals.

For the PSIQ, there were 334 participants (276 females and 58 males) from Florida with a mean age of 20.5 years, and these participants also performed the VVIQ-2. There were 217 participants in the London dataset, which from Clark & Maguire (2023)⁶⁷, with a mean age of 29 years and comprising 109 females and 108 males, available here:

<https://datadryad.org/dataset/doi:10.5061/dryad.2v6wwpzt3>. We also analyzed the data by pooling all the data from the “Florida + London” group, which comprised 551 participants. For more details on the Polish and London datasets, the readers are advised to look at the Jankowska & Karwowski (2022) and Clark & Maguire (2023) publications, respectively. In each population, participants either performed the VVIQ-2 or the PSIQ questionnaires, as instructed. Polish data was obtained from participants doing the Polish translated version of VVIQ-2. In contrast, all the other populations performed the imagination surveys in the original English version. We did not have a prior sample size for our main psychological network analysis, rather we computed CS-coefficient (discussed below) to estimate the reliability of centrality measures. The compiled data is available on OSF (<https://osf.io/658kw>) for the current work.

AI Models

We used six models in total, with four from the Gemma3 family and two models from the Llama family. From the Gemma3 family, we utilized models with 12 and 27 billion parameters, along with their corresponding quantization-aware trained models (postfixed as QAT). Quantized models often reduce model size without changing the number of parameters and quality of responses by lowering the decimal precision of the model weights, enabling us to compare models across different training regimes while keeping the model architecture constant. For more information about the quantization-aware training, readers are recommended to refer to Jacob et al., (2017)⁶⁸. From the Llama family, we used Llama-3.3, which has 70 billion parameters, and

Llama-4.0-Scout (16x17b), a model that combines an expert's model with 16 experts and 17 billion parameters each. Thus, each model offers a distinct type of long-term memory, based on its training regime and architecture. All models were run locally using one NVIDIA B100 GPU.

Imagination Tasks

The VVIQ-2 and PSIQ ask participants to rate the vividness of their imagination on a scale of 1 to 5 and 0 to 10, respectively, for a given item prompt. We assume that vividness ratings capture a psychological experience based on the perceived vividness of the internal world. The VVIQ-2 consists of eight contexts with four items each with 32 items in total. We used three items in each of the PSIQ's contexts, with 21 total imagination prompts. We hypothesized that the vividness ratings may exhibit structural characteristics due to the internal world model, organized similarly across human populations. However, in the current investigation, we utilized the VVIQ-2 and PSIQ as tools to sample the internal world model using imagination prompts and vividness ratings, and measure the structural aspects of human and LLM imagination using psychological network science. Inherently, the VVIQ-2 and PSIQ are structurally clustered and organized based on different contexts (8 contexts in VVIQ-2 and 7 contexts in PSIQ, as mentioned above). Additionally, the VVIQ-2 contexts focus solely on the visual aspects of the external world, whereas the PSIQ contexts sample the ability to generate and experience sensory imagery across multiple modalities.

For the simulation of LLM responses, the English version of the imagination questionnaires was converted into JSON format and can be found on the OSF (<https://osf.io/658kw>). AI model providers frequently use JSON to format text for training the LLM models⁶⁹. Using explicit output parsers, our LLMs were constrained to provide only vividness responses, and with our LLM-based AI models, we performed the imagination task in

two ways: (1) independently and (2) cumulatively. In the independent condition, LLM models responded to each context and prompt without recalling previous trials, treating each item as independent of the others as instructed to the participants. During the cumulative condition, LLM models had access to previous interactions and values; thus, only the first item in this condition did not have information about the past, while subsequent items had a memory of past interactions with items/prompts and their own vividness rating. Thus, our two tasks allowed us to simulate vividness ratings with either (1) independence of previous trials, or (2) having previous trial memory, in LLM models for simulation.

The system message to each LLM call was provided in the following format:

{*“You are a helpful assistant with the following individual characteristics:*

<definition of imagination ability> <persona statements>

Perform the task as per the instructions described below.

TASK CONTEXT: <instructions>” }

An example trial for the VVIQ-2 given to the LLM looked like the following:

“{"TRIAL_CONTEXT": "Think of the rising sun. Consider carefully the picture that comes before your mind's eye.", "TRIAL": "A rainbow appears."}”. The trial context and message changed depending on the questionnaire. An example trial for the PSIQ looked like: *“Imagine the appearance of a bonfire. How vivid is the image?”*

The instructions in the task context above were similar to the instructions provided to human participants for the imagination questionnaire. The items from the imagination questionnaire were provided as human/user messages with their item context. The item from each questionnaire to the LLM was provided as Human/User messages for the LLMs to provide

the vividness rating as responses in JSON format: {Vividness: x}, depending on the scale of the given imagination questionnaire.

Each model was used to simulate 200 personas randomly sampled from the Persona-Chat dataset⁴² across five levels of imagination ability characteristics. To simulate different imagination abilities, we manipulated them across five levels: (a) no imagination ability prompt; (b) typical imagery: *“Typical imagery is a standard mental imagery capacity most people have. It allows for moderately vivid and detailed mental pictures. Individuals with typical imagery can summon clear, detailed images in their mind's eye but might not be able to sustain them for long periods or with photographic precision.”*; (c) aphantasia: *“Aphantasia is inability to form mental images, even when attempting to do so. Individuals with aphantasia typically describe a “blank mind's eye” when asked to imagine something, such as a loved one's face or a scene.”*; (d) hypophantasia: *“Hypophantasia is reduced ability to form mental images. Visualizations may exist but are vague, dim, or not detailed. Individuals with hypophantasia may perceive faint or blurry images but lacks the richness and clarity of typical imagery.”*; and (e) hyperphantasia: *“Hyperphantasia is the ability to form extremely vivid, lifelike mental images that are nearly indistinguishable from actual vision. Individuals with hyperphantasia may report “seeing” images as if they were real, with high detail, colors, and sometimes motion.”* When no imagination ability prompt was given, only the persona statements were provided with the task instructions, as in the VVIQ-2 or PSIQ questionnaire. For the simulations involving all other imagination ability characteristics, persona statements were prefixed to the definition of the imagination ability. Thus, in total, for a type of task (independent or cumulative), 1000 simulations were generated from each LLM model, with 200 simulations for each of the five imagination ability instruction conditions. The total vividness score from the VVIQ-2 was

analyzed using JASP (0.19.3) to investigate the effects of LLM task type (cumulative or independent), imagination ability prompt, and model (Fig. 1A). Kruskal-Wallis and Dunn's post-hoc tests were performed for between-group comparisons, and two-tailed p-values are reported in the Results section. We did not have a hypothesis for the total vividness score, other than anticipating that imagination ability prompts for aphantasia would cause total vividness scores to be lower, and hyperphantasia prompts would cause vividness scores to be higher compared to the typical imagery instruction or no imagination ability instruction.

AI Population Diversity Sampling

For constructing the imagination networks from each of the LLM responses, we created a population of LLM simulations based on human imagination abilities by downsampling 1000 simulations from across imagination abilities to 600 total simulations for each of the LLMs. The human population consists of individuals with varying imagination abilities, as measured using the total vividness score given a questionnaire. We first extracted the quantile ranges using every 10th percentile of the total vividness scores from the pooled human data from the VVIQ-2 (Florida + Poland group) and PSIQ (Florida + London group). For each LLM simulation, given the model and questionnaire, the total vividness score was computed. LLM simulations were selected based on the human quantile ranges, and from each quantile range, 60 LLM simulations were randomly chosen. Whenever there were not enough simulations for a given quantile range, all simulations were selected within the given quantile range. The remaining simulations for that quantile were chosen from outside the quantile range and removed from the overall samples for further sampling. Thus, after population diversity sampling, we had 600 simulations from each of the models for the given task (independent or cumulative) and imagination questionnaire (VVIQ-2 or PSIQ), which were used to create imagination networks.

Additionally, an important reason to perform AI population diversity sampling is that differences in imagination abilities could explain the topological regularities observed in human imagination networks. Diversifying AI simulations based on imagination ability from human data helps us introduce statistical variances for the LLM-based imagination networks, which can represent the distribution of human imagination across different imagination abilities. Total vividness scores for the VVIQ-2 data were analyzed for different populations from human groups and LLM models after population diversity sampling (Fig. 1B) using Kolmogorov-Smirnov (K-S) tests with Benjamini/Hochberg FDR corrections for multiple comparisons, with two-tailed p-values reported. The code can be found on GitHub (https://github.com/saurabhr/imagine_world_model).

Network Analysis

By performing network analysis of vividness ratings, we can investigate the internal world model of characterizing how one experiences their environment in day-to-day activities using reproductive imagination. We constructed the edge weights between two nodes (scenes) to represent the associations between them, thus creating an imagination network representing the internal worlds in the two tasks. Therefore, the node represents the state of the world, and edges represent the association between those states that are solely defined by the imagination in an individual's mind, proposed as imagination networks in the current investigation.

Different network measurements represent how the information is processed in the networks. Given a specific imagination network, we characterized the IWM of a human or AI agent using micro-level network centrality of each node, which reveals the importance of each node in a given network. Although there are numerous centrality measures in network science, we focused on four common psychological network centrality measures: expected influence,

strength, closeness, and betweenness⁴⁰ using the bootnet library⁷⁰ in R. In our study, we correlated the different centralities of nodes of an imagination network with those from all other networks to investigate whether each imagined scenario held similar importance across the various networks for a given imagination questionnaire. If a centrality measure for the nodes in an imagined network correlated with another imagined network, we inferred that the imagined scenario was similarly involved across the networks in the overall topology of imagination networks that represent the internal world model. Thus, a positive high correlation of a centrality measure of nodes across imagination networks indicates that the internal world model is similarly utilized across a given type of imagination network.

We performed post-hoc stability analysis; specifically, we computed the CS-coefficient using the bootnet library with a case-dropping value of 500 and a bootstrap value of 5000 for the centrality measurements to establish their robustness and accuracy. Centrality stability is preferred to be above 0.5, or at least above 0.25⁴³. The CS-coefficient (centrality stability) effectively measures the proportion of data that can be eliminated while ensuring, with 95% confidence, that a correlation of at least 0.7 is maintained with the original centrality measures⁴³. See Supplementary Table S1 for VVIQ-2 and Table S2 for PSIQ for CS-coefficient results. We investigated whether positive correlations for centrality measures would emerge due to similar world models between agents, and report pairwise Pearson's r correlations and one-tailed p-values. Whenever pairwise normality was violated, we provided Spearman's ρ correlations. Further, we also reported Benjamini/Hochberg FDR corrections for multiple comparisons for the p-values.

The vividness ratings are ordinal scale data for which polychoric partial correlations⁴³ should be preferred, as they assume a latent distribution underlying the ordinal scale value.

However, our initial investigations failed to find stable centrality measures in networks, primarily for the LLMs. Thus, the Spearman method was used for partial correlations in EBICglasso for estimating the imagination networks⁴³. To investigate whether nodes had similar influences across networks, depending on the type of centrality measures, we performed pairwise correlations between the centralities of nodes across networks.

To understand how different items are in the data clusters based on the associations of vividness ratings between them, we performed clustering analysis using the walktrap community⁴⁴ detection algorithm with the LE method in the EGANet library⁷¹ in R. The results presented here are robust to type of community detection algorithm as in our preliminary analysis we utilized different algorithm (TMFG)⁷² and found similar results⁷³. The similarity in cluster assignments of different nodes across the networks was calculated using the adjusted rand score from the sklearn library⁷⁴ in Python. The higher the adjusted rand-score, the higher the clustering alignment across networks

Each network was computed using the bootnet library⁷⁰ in the R programming language based on the EBICglasso method with a commonly used common tuning parameter of 0.5 using the vividness ratings for each item. The EBICglasso method promotes fewer connections between network nodes by combining Graphical LASSO and the Extended Bayesian Information Criterion for model selection (EBICglasso), incorporating partial correlations, which results in fewer false-positive edges in the network compared to networks formed solely using partial correlations⁴³. See Table S1, S2 for clustering assignment for each node for VVIQ-2, and PSIQ imagination networks respectively. The code can be found on GitHub (https://github.com/saurabhr/imagine_world_model).

References

1. Chollet, F. On the Measure of Intelligence. Preprint at <https://doi.org/10.48550/arXiv.1911.01547> (2019).
2. Hassabis, D., Kumaran, D., Summerfield, C. & Botvinick, M. Neuroscience-Inspired Artificial Intelligence. *Neuron* **95**, 245–258 (2017).
3. Lake, B. M., Ullman, T. D., Tenenbaum, J. B. & Gershman, S. J. Building machines that learn and think like people. *Behav. Brain Sci.* **40**, e253 (2017).
4. Buckner, R. L. & Carroll, D. C. Self-projection and the brain. *Trends Cogn. Sci.* **11**, 49–57 (2007).
5. Kosslyn, S. M., Thompson, W. L. & Ganis, G. *The Case for Mental Imagery*. vi, 248 (Oxford University Press, New York, NY, US, 2006).
doi:10.1093/acprof:oso/9780195179088.001.0001.
6. Schacter, D. L. *et al.* The Future of Memory: Remembering, Imagining, and the Brain. *Neuron* **76**, 677–694 (2012).
7. Sutton, R. S. & Barto, A. *Reinforcement Learning: An Introduction*. (The MIT Press, Cambridge, Massachusetts London, England, 2020).
8. Silver, D., Singh, S., Precup, D. & Sutton, R. S. Reward is enough. *Artif. Intell.* **299**, 103535 (2021).
9. Ha, D. & Schmidhuber, J. World Models. <https://doi.org/10.5281/zenodo.1207631> (2018)
doi:10.5281/zenodo.1207631.
10. Gershman, S. J., Zhou, J. & Kommer, C. Imaginative Reinforcement Learning: Computational Principles and Neural Mechanisms. *J. Cogn. Neurosci.* **29**, 2103–2113 (2017).

11. Balaban, H. & Ullman, T. D. The capacity limits of moving objects in the imagination. *Nat. Commun.* **16**, 5899 (2025).
12. Smallwood, J. & Schooler, J. W. The Science of Mind Wandering: Empirically Navigating the Stream of Consciousness. *Annu. Rev. Psychol.* **66**, 487–518 (2015).
13. Christoff, K., Irving, Z. C., Fox, K. C. R., Spreng, R. N. & Andrews-Hanna, J. R. Mind-wandering as spontaneous thought: a dynamic framework. *Nat. Rev. Neurosci.* **17**, 718–731 (2016).
14. Abraham, A. The imaginative mind. *Hum. Brain Mapp.* **37**, 4197–4211 (2016).
15. Vafa, K., Chen, J. Y., Rambachan, A., Kleinberg, J. & Mullainathan, S. Evaluating the world model implicit in a generative model. *Adv. Neural Inf. Process. Syst.* **37**, 26941–26975 (2024).
16. Jin, C. & Rinard, M. Emergent representations of program semantics in language models trained on programs. in *Forty-first International Conference on Machine Learning* (2024).
17. Kahn, A. E. & Daw, N. D. Humans rationally balance detailed and temporally abstract world models. *Commun. Psychol.* **3**, 1 (2025).
18. Yildirim, I. & Paul, L. A. From task structures to world models: what do LLMs know? *Trends Cogn. Sci.* **28**, 404–415 (2024).
19. Gao, Q. *et al.* Do Vision-Language Models Have Internal World Models? Towards an Atomic Evaluation. Preprint at <https://doi.org/10.48550/arXiv.2506.21876> (2025).
20. Ding, J. *et al.* Understanding World or Predicting Future? A Comprehensive Survey of World Models. Preprint at <https://doi.org/10.48550/arXiv.2411.14499> (2025).
21. Diester, I. *et al.* Internal world models in humans, animals, and AI. *Neuron* **112**, 2265–2268 (2024).

22. Jin, C. & Rinard, M. Emergent Representations of Program Semantics in Language Models Trained on Programs. Preprint at <https://doi.org/10.48550/arXiv.2305.11169> (2024).
23. Daw, N. D., Niv, Y. & Dayan, P. Uncertainty-based competition between prefrontal and dorsolateral striatal systems for behavioral control. *Nat. Neurosci.* **8**, 1704–1711 (2005).
24. Gershman, S. J., Horvitz, E. J. & Tenenbaum, J. B. Computational rationality: A converging paradigm for intelligence in brains, minds, and machines. *Science* **349**, 273–278 (2015).
25. Matsuo, Y. *et al.* Deep learning, reinforcement learning, and world models. *Neural Netw.* **152**, 267–275 (2022).
26. Ranjan, S. & Odegaard, B. Heterarchy or hierarchy? Insights from a new model of visual imagination. *Phys. Life Rev.* **49**, 74–76 (2024).
27. Spagna, A. *et al.* Competing models of visual mental imagery: Reverse hierarchy or heterarchy? *Phys. Life Rev.* **51**, 96–100 (2024).
28. Spagna, A. *et al.* Visual mental imagery: Evidence for a heterarchical neural architecture. *Phys. Life Rev.* **48**, 113–131 (2024).
29. Schwarzkopf, D. S. *et al.* Vividness of mental imagery is a broad trait measure of internally generated visual experiences. 2025.09.30.679629 Preprint at <https://doi.org/10.1101/2025.09.30.679629> (2025).
30. Marks, D. F. New directions for mental imagery research. *J. Ment. Imag.* **19**, 153–167 (1995).
31. Andrade, J., May, J., Deeprose, C., Baugh, S.-J. & Ganis, G. Assessing vividness of mental imagery: The Plymouth Sensory Imagery Questionnaire. *Br. J. Psychol.* **105**, 547–563 (2014).

32. Wang, S. L., Isola, P. & Cheung, B. Words That Make Language Models Perceive. Preprint at <https://doi.org/10.48550/arXiv.2510.02425> (2025).
33. Bommasani, R. *et al.* On the Opportunities and Risks of Foundation Models. Preprint at <https://doi.org/10.48550/arXiv.2108.07258> (2022).
34. Andreas, J. Language Models as Agent Models. Preprint at <https://doi.org/10.48550/arXiv.2212.01681> (2022).
35. Newman, M. Networks: an introduction. 2010. *United States Oxf. Univ. Press Inc N. Y.* 1–2 (2010).
36. Robinaugh, D. J., Millner, A. J. & McNally, R. J. Identifying highly influential nodes in the complicated grief network. *J. Abnorm. Psychol.* **125**, 747–757 (2016).
37. Bringmann, L. F. *et al.* What do centrality measures measure in psychological networks? *J. Abnorm. Psychol.* **128**, 892–903 (2019).
38. Epskamp, S., Borsboom, D. & Fried, E. I. Estimating psychological networks and their accuracy: A tutorial paper. *Behav. Res. Methods* **50**, 195–212 (2018).
39. Blondel, V. D., Guillaume, J.-L., Lambiotte, R. & Lefebvre, E. Fast unfolding of communities in large networks. *J. Stat. Mech. Theory Exp.* **2008**, P10008 (2008).
40. Borsboom, D. *et al.* Network analysis of multivariate data in psychological science. *Nat. Rev. Methods Primer* **1**, 1–18 (2021).
41. Borsboom, D. & Cramer, A. O. Network analysis: an integrative approach to the structure of psychopathology. *Annu. Rev. Clin. Psychol.* **9**, 91–121 (2013).
42. Zhang, S. *et al.* Personalizing Dialogue Agents: I have a dog, do you have pets too? in *Proceedings of the 56th Annual Meeting of the Association for Computational Linguistics*

- (*Volume 1: Long Papers*) (eds Gurevych, I. & Miyao, Y.) 2204–2213 (Association for Computational Linguistics, Melbourne, Australia, 2018). doi:10.18653/v1/P18-1205.
43. Epskamp, S. & Fried, E. I. A tutorial on regularized partial correlation networks. *Psychol. Methods* **23**, 617–634 (2018).
 44. Pons, P. & Latapy, M. Computing communities in large networks using random walks. in *International symposium on computer and information sciences* 284–293 (Springer, 2005).
 45. Fortunato, S. Community detection in graphs. *Phys. Rep.* **486**, 75–174 (2010).
 46. Schacter, D. L. & Addis, D. R. The cognitive neuroscience of constructive memory: remembering the past and imagining the future. *Philos. Trans. R. Soc. B Biol. Sci.* **362**, 773–786 (2007).
 47. Hassabis, D. & Maguire, E. A. The construction system of the brain. *Philos. Trans. R. Soc. B Biol. Sci.* **364**, 1263–1271 (2009).
 48. Fazekas, P. Vividness and content. *Mind Lang.* **39**, 61–79 (2024).
 49. Morales, J. Mental strength: A theory of experience intensity. *Philos. Perspect.* **37**, 248–268 (2023).
 50. Langkau, J. Two Kinds of Imaginative Vividness. *Can. J. Philos.* **51**, 33–47 (2021).
 51. Marjeh, R., Sucholutsky, I., van Rijn, P., Jacoby, N. & Griffiths, T. L. Large language models predict human sensory judgments across six modalities. *Sci. Rep.* **14**, 21445 (2024).
 52. Loconte, R., Russo, R., Capuozzo, P., Pietrini, P. & Sartori, G. Verbal lie detection using Large Language Models. *Sci. Rep.* **13**, 22849 (2023).
 53. Kawakita, G., Zeleznikow-Johnston, A., Tsuchiya, N. & Oizumi, M. Comparing Color Similarity Structures between Humans and LLMs via Unsupervised Alignment. *arXiv.org* <https://arxiv.org/abs/2308.04381v1> (2023).

54. Mahowald, K. *et al.* Dissociating language and thought in large language models: a cognitive perspective. <https://doi.org/10.48550/arXiv.2301.06627> (2023)
doi:10.48550/arXiv.2301.06627.
55. Pezzulo, G., Parr, T., Cisek, P., Clark, A. & Friston, K. Generating meaning: active inference and the scope and limits of passive AI. *Trends Cogn. Sci.* **28**, 97–112 (2024).
56. Richens, J., Abel, D., Bellot, A. & Everitt, T. General agents contain world models. Preprint at <https://doi.org/10.48550/arXiv.2506.01622> (2025).
57. Wyble, B., Tam, J., Deal, I. & Bowman, H. Understanding the flexibility of working memory: Compositionality, generative processing, anchors and holistic representations. *Neurosci. Biobehav. Rev.* **179**, 106387 (2025).
58. Harnad, S. The symbol grounding problem. *Phys. Nonlinear Phenom.* **42**, 335–346 (1990).
59. Barsalou, L. W. Grounded Cognition. *Annu. Rev. Psychol.* **59**, 617–645 (2008).
60. Seth, A. K. & Bayne, T. Theories of consciousness. *Nat. Rev. Neurosci.* **23**, 439–452 (2022).
61. Seth, A. K. Conscious artificial intelligence and biological naturalism. *Behav. Brain Sci.* 1–42 (2025) doi:10.1017/S0140525X25000032.
62. Dehaene, S., Lau, H. & Kouider, S. What is consciousness, and could machines have it? *Robot. AI Humanity Sci. Ethics Policy* 43–56 (2021).
63. Dijkstra, N. & Fleming, S. M. Subjective signal strength distinguishes reality from imagination. *Nat. Commun.* **14**, 1627 (2023).
64. Gonsalves, B. *et al.* Neural Evidence That Vivid Imagining Can Lead to False Remembering. *Psychol. Sci.* **15**, 655–660 (2004).
65. Singhal, I. & Srivastava, N. Dynamics of mental imagery. *Conscious. Cogn.* **131**, 103865 (2025).

66. Jankowska, D. M. & Karwowski, M. How Vivid Is Your Mental Imagery? *Eur. J. Psychol. Assess.* **39**, 437–448 (2023).
67. Clark, I. A. & Maguire, E. A. Release of cognitive and multimodal MRI data including real-world tasks and hippocampal subfield segmentations. *Sci. Data* **10**, 540 (2023).
68. Jacob, B. *et al.* Quantization and Training of Neural Networks for Efficient Integer-Arithmetic-Only Inference. Preprint at <https://doi.org/10.48550/arXiv.1712.05877> (2017).
69. He, J. *et al.* Does Prompt Formatting Have Any Impact on LLM Performance? Preprint at <https://doi.org/10.48550/arXiv.2411.10541> (2024).
70. Epskamp, S. & Fried, E. I. Package ‘bootnet’. (2025).
71. Golino, H. & Christensen, A. *EGAnet: Exploratory Graph Analysis – A Framework for Estimating the Number of Dimensions in Multivariate Data Using Network Psychometrics.* (2025). doi:10.32614/CRAN.package.EGAnet.
72. Massara, G. P., Di Matteo, T. & Aste, T. Network filtering for big data: Triangulated maximally filtered graph. *J. Complex Netw.* **5**, 161–178 (2016).
73. Ranjan, S. & Odegaard, B. Visual Imagination Networks in Humans and Large Language Models. *J. Vis.* **25**, 2709–2709 (2025).
74. Buitinck, L. *et al.* API design for machine learning software: experiences from the scikit-learn project. in *ECML PKDD Workshop: Languages for Data Mining and Machine Learning* 108–122 (2013).

Supplementary Material

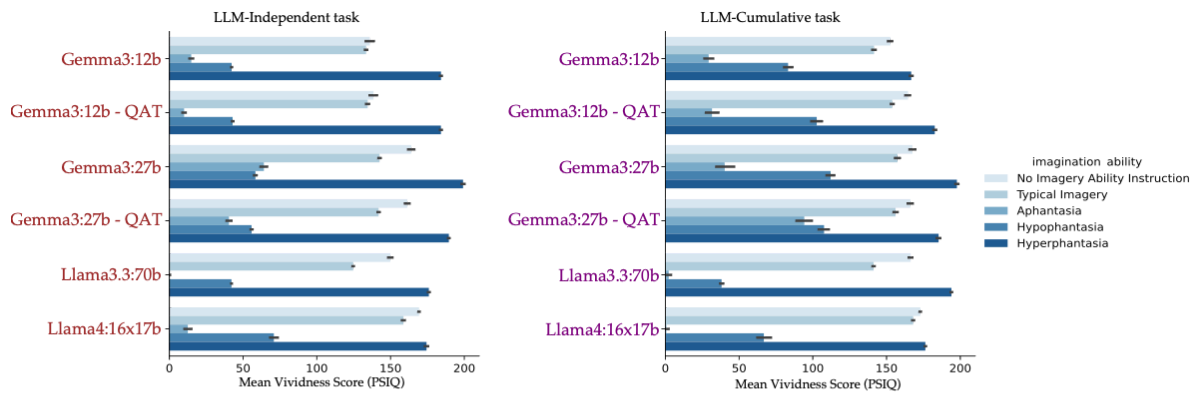
Internal World Models as Imagination Networks in Cognitive Agents

Saurabh Ranjan and Brian Odegaard

Department of Psychology, University of Florida

Address correspondence to: ranjan.saurabh@outlook.com, bodegaard@ufl.edu

A. LLM's mean vividness across imagination ability.



B. Mean (left) and distribution (right) of total vividness score in Humans and after population diversity sampling in LLMs.

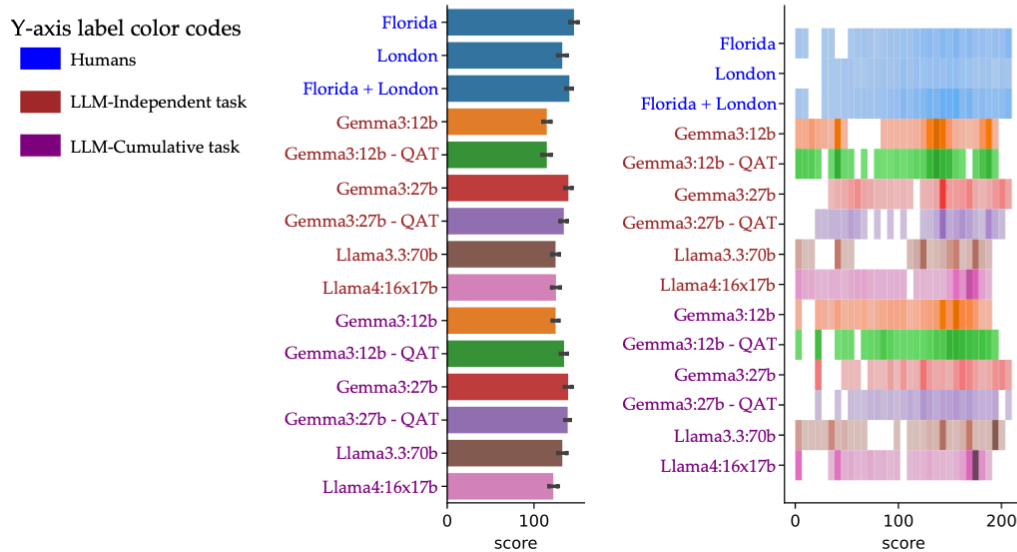


Fig. S1. Total vividness scores and distributions in LLMs and Humans using the PSIQ. (A) Total vividness score with prompt about different imagination ability statements on the LLM simulation for PSIQ. (B) (*Left*) Mean vividness scores in human populations and after population diversity sampling (*see methods*) for each of the LLMs based on the total vividness score of the simulations for PSIQ. (*Right*) Distribution of the total vividness score in humans and after population diversity sampling for each of the LLMs for PSIQ. The error bars in bar plots are bootstrapped ($N = 1000$) 95% confidence intervals.

Table S1. CS-Coefficient of nodes for VVIQ-2 imagination networks in different cognitive agents.

Groups	Betweenness	Closeness	Expected Influence	Strength
Florida	0.42	0.47	0.69	0.57
Poland 1	0.21	0.48	0.71	0.71
Poland 2	0.27	0.45	0.75	0.75
Poland All	0.29	0.52	0.75	0.75
Florida +Poland	0.43	0.73	0.75	0.75
Gemma3:12b_i	0.42	0.42	0.75	0.68
Gemma3:12b-QAT_i	0.18	0.27	0.75	0.75
Gemma3:27b_i	0.21	0.44	0.75	0.75
Gemma3:27b-QAT_i	0.19	0.32	0.75	0.73
Llama3.3:70b_i	0.18	0.31	0.75	0.75
Llama4:16x17b_i	0.39	0.6	0.75	0.65
Gemma3:12b_c	0.39	0.61	0.75	0.67
Gemma3:12b-QAT_c	0.63	0.38	0.75	0.72
Gemma3:27b_c	0.49	0.6	0.75	0.65
Gemma3:27b-QAT_c	0.19	0.32	0.75	0.73
Llama3.3:70b_c	0.44	0.48	0.75	0.75
Llama4:16x17b_c	0.55	0.74	0.75	0.75

Note: CS-Coefficient should ideally be more than 0.50 or at least 0.25 (Epskamp & Fried, 2018). Values are rounded to two decimal places. The postfixes “_i” and “_c” to LLM models denote LLM-independent and LLM-Cumulative tasks, respectively.

Table S2. CS-Coefficient of nodes for PSIQ imagination networks in different cognitive agents.

Groups	Betweenness	Closeness	Expected Influence	Strength
Florida	0.08	0.4	0.66	0.58
London	0	0.18	0.63	0.45
Florida+London	0.2	0.68	0.75	0.72
Gemma3:12b_i	0.35	0.43	0.75	0.75
Gemma3:12b-QAT_i	0.42	0.35	0.74	0.73
Gemma3:27b_i	0.49	0.74	0.75	0.74
Gemma3:27b-QAT_i	0.33	0.66	0.75	0.74
Llama3.3:70b_i	0.42	0.49	0.75	0.75
Llama4:16x17b_i	0.25	0.61	0.75	0.74
Gemma3:12b_c	0.62	0.64	0.75	0.75
Gemma3:12b-QAT_c	0.14	0.57	0.75	0.75
Gemma3:27b_c	0.58	0.71	0.75	0.68
Gemma3:27b-QAT_c	0.49	0.74	0.75	0.74
Llama3.3:70b_c	0.56	0.58	0.75	0.74
Llama4:16x17b_c	0.25	0.31	0.75	0.29

Note: CS-Coefficient should ideally be more than 0.50 or at least 0.25 (Epskamp & Fried, 2018). Values are rounded to two decimal places. The postfixes “_i” and “_c” to LLM models denote LLM-independent and LLM-Cumulative tasks, respectively.

Table S3. Clusters assignments of nodes for VVIQ-2 imagination networks in different cognitive agents.

NODES	Florida	Poland-1	Poland-2	Poland-All	Florida + Poland	Gemma3:12 _i	Gemma3:12 -QAT_i	Gemma3:27 _i	Gemma3:27 -QAT_i	Llama3.3:70 b_i	Llama4:16x1 7b_i	Gemma3:12 _c	Gemma3:12 -QAT_c	Gemma3:27 _c	Gemma3:27 -QAT_c	Llama3.3:70 b_c	Llama4:16x1 7b_c
A_1	1	1	1	1	1	1	1	1	1	1	1	1	1	1	1	1	1
A_2	1	1	1	1	1	1	1	1	1	1	1	2	1	2	2	1	1
A_3	1	1	1	1	1	1	1	1	1	1	1	2	1	2	2	1	2
A_4	1	1	1	1	1	1	1	1	1	1	1	1	1	1	2	1	1
B_1	2	2	2	2	2	1	1	1	1	1	2	3	1	1	3	1	2
B_2	2	1	2	3	2	1	1	1	1	1	2	3	1	1	3	1	2
B_3	2	3	3	2	3	1	1	1	1	1	3	4	1	3	4	1	2
B_4	2	3	3	2	3	1	1	1	1	1	2	4	1	1	4	1	2
C_1	3	1	4	1	1	1	1	1	1	1	3	1	1	1	1	1	3
C_2	3	1	4	1	1	1	1	1	1	1	1	3	1	1	3	1	1
C_3	3	1	4	1	1	1	1	1	1	1	3	1	1	1	5	1	3
C_4	3	1	4	1	1	1	1	1	1	1	1	2	1	3	5	1	1
D_1	4	2	2	3	2	1	1	1	1	1	2	3	1	1	1	1	2
D_2	4	2	2	3	2	1	1	1	1	1	3	3	1	1	3	1	4
D_3	4	2	2	3	2	1	1	1	1	1	3	1	1	4	4	1	4
D_4	4	3	3	2	3	1	1	1	1	1	3	4	1	3	4	1	2
E_1	3	2	3	2	3	1	1	1	1	1	1	1	1	1	1	1	1
E_2	3	2	3	2	3	1	1	1	1	1	3	2	1	3	5	1	1
E_3	3	3	3	2	3	1	1	1	1	1	2	2	1	3	5	1	1
E_4	3	3	3	2	3	1	1	1	1	1	2	2	1	1	5	1	1
F_1	3	2	2	3	2	1	1	1	1	1	2	3	1	4	3	1	2
F_2	3	3	2	2	3	1	1	1	1	1	2	3	1	3	4	1	3
F_3	3	3	3	2	3	1	1	1	1	1	2	4	1	1	4	1	2
F_4	3	3	3	2	3	1	1	1	1	1	2	4	1	3	5	1	3
G_1	5	4	5	4	4	1	1	1	1	1	1	1	1	1	1	1	3
G_2	5	4	5	4	4	1	1	1	1	1	1	1	1	1	5	1	3
G_3	5	4	5	4	4	1	1	1	1	1	1	2	1	3	5	1	3
G_4	5	4	5	4	4	1	1	1	1	1	1	1	1	3	5	1	3
H_1	6	5	6	3	5	1	1	1	1	1	3	3	1	1	1	1	4
H_2	6	5	6	3	5	1	1	1	1	1	3	3	1	4	3	1	3
H_3	6	5	6	3	5	1	1	1	1	1	3	3	1	4	3	1	4
H_4	6	5	6	2	5	1	1	1	1	1	3	4	1	3	4	1	3

Table S4. Clusters assignments of nodes for PSIQ imagination networks in different cognitive agents.

NODES	Florida	London	Florida + London	Gemma3:1 2_i	Gemma3:1 2-QAT_i	Gemma3:1 7_j	Gemma3:2 7-QAT_i	Llama3.3:7 0b_j	Llama4:16x 17b_j	Gemma3:1 2_c	Gemma3:1 2-QAT_c	Gemma3:2 7_c	Gemma3:2 7-QAT_c	Llama3.3:7 0b_c	Llama4:16x 17b_c
App_1	1	1	1	1	1	1	1	1	1	1	1	1	1	1	1
App_2	1	1	1	1	1	1	1	1	1	1	1	1	1	1	1
App_3	1	1	1	1	1	1	1	1	1	1	1	1	1	1	1
So_1	2	1	2	1	1	1	1	1	1	1	1	1	1	2	1
So_2	2	1	2	1	1	1	1	1	1	1	1	1	1	2	1
So_3	2	1	2	1	1	1	1	1	1	1	1	1	1	2	1
Sm_1	3	2	3	1	1	1	1	1	1	1	1	1	1	3	1
Sm_2	3	2	3	1	1	1	1	1	1	1	1	1	1	3	1
Sm_3	3	2	3	1	1	1	1	1	1	1	1	1	1	3	1
Ta_1	3	2	3	1	1	1	1	1	1	1	1	1	1	4	1
Ta_2	3	2	3	1	1	1	1	1	1	1	1	1	1	4	1
Ta_3	3	2	3	1	1	1	1	1	1	1	1	1	1	5	1
To_1	4	3	4	1	1	1	1	1	1	1	1	1	1	3	1
To_2	4	3	4	1	1	1	1	1	1	1	1	1	1	3	1
To_3	4	3	4	1	1	1	1	1	1	1	1	1	1	3	1
Bo_1	4	3	4	1	1	1	1	1	1	1	1	1	1	3	1
Bo_2	4	3	4	1	1	1	1	1	1	1	1	1	1	3	1
Bo_3	4	3	4	1	1	1	1	1	1	1	1	1	1	3	1
Fe_1	5	4	5	1	1	1	1	1	1	1	1	1	1	5	1
Fe_2	5	4	5	1	1	1	1	1	1	1	1	1	1	5	1
Fe_3	5	4	5	1	1	1	1	1	1	1	1	1	1	5	1

Table S5. Cluster alignment of nodes for VVIQ-2 imagination networks in different cognitive agents using adjusted rand index (ARI).

Groups	Florida	Poland-1	Poland-2	Poland-All	Florida + Poland	Gemma3:12_j	Gemma3:12-QAT_j	Gemma3:27_j	Gemma3:27-QAT_j	Llama3.3:70_b_j	Llama4:16x17b_j	Gemma3:12_c	Gemma3:12-QAT_c	Gemma3:27_c	Gemma3:27-QAT_c	Llama3.3:70_b_c	Llama4:16x17b_c
Florida	1	0.285951	0.402658	0.266272	0.389664	0	0	0	0	0.157068	0.016157	0	0.007047	0.121667	0	0.20064	
Poland-1	0.285951	1	0.548929	0.559838	0.752988	0	0	0	0	0.205748	0.132181	0	0.05317	0.105831	0	0.104084	
Poland-2	0.402658	0.548929	1	0.56338	0.791019	0	0	0	0	0.201618	0.223963	0	0.029583	0.155482	0	0.145438	
Poland-All	0.266272	0.559838	0.56338	1	0.750549	0	0	0	0	0.216749	0.23624	0	0.109957	0.174556	0	0.141407	
Florida + Poland	0.389664	0.752988	0.791019	0.750549	1	0	0	0	0	0.225974	0.169722	0	0.07227	0.148072	0	0.163799	
Gemma3:12_j	0	0	0	0	0	1	1	1	1	1	0	0	1	0	0	1	0
Gemma3:12-QAT_j	0	0	0	0	0	1	1	1	1	1	0	0	1	0	0	1	0
Gemma3:27_j	0	0	0	0	0	1	1	1	1	1	0	0	1	0	0	1	0
Gemma3:27-QAT_j	0	0	0	0	0	1	1	1	1	1	0	0	1	0	0	1	0
Llama3.3:70b_j	0	0	0	0	0	1	1	1	1	1	0	0	1	0	0	1	0
Llama4:16x17b_j	0.157068	0.205748	0.201618	0.216749	0.225974	0	0	0	0	1	0.104965	0	-0.015945	0.020942	0	0.124922	
Gemma3:12_c	0.016157	0.132181	0.223963	0.23624	0.169722	0	0	0	0	0.104965	1	0	0.119578	0.350067	0	0.120743	
Gemma3:12-QAT_c	0	0	0	0	0	1	1	1	1	1	0	0	1	0	0	1	0
Gemma3:27_c	0.007047	0.05317	0.029583	0.109957	0.07227	0	0	0	0	-0.015945	0.119578	0	1	0.165919	0	-0.00623	
Gemma3:27-QAT_c	0.121667	0.105831	0.155482	0.174556	0.148072	0	0	0	0	0.020942	0.350067	0	0.165919	1	0	0.072276	
Llama3.3:70b_c	0	0	0	0	0	1	1	1	1	1	0	0	1	0	0	1	0
Llama4:16x17b_c	0.20064	0.104084	0.145438	0.141407	0.163799	0	0	0	0	0.124922	0.120743	0	-0.00623	0.072276	0	1	

Note: Computed pairwise for each imagination network. The above matrix is symmetrical across the diagonal. The postfixes “_i” and “_c” to LLM models denote LLM-Independent and LLM-Cumulative tasks, respectively.

Table S6. Cluster alignment of nodes for PSIQ based imagination networks in different cognitive agents using adjusted rand index (ARI).

Groups	Florida	London	Florida +London	Gemma3:12_ i	Gemma3:12_ QAT_i	Gemma3:27_ i	Gemma3:27_ QAT_i	Llama3.3:70 b_i	Llama4:16x1 7b_i	Gemma3:12_ c	Gemma3:12_ QAT_c	Gemma3:27_ c	Gemma3:27_ QAT_c	Llama3.3:70 b_c	Llama4:16x1 7b_c	
Florida	1	0.869888	1	0	0	0	0	0	0	0	0	0	0	0.541547	0	0
London	0.869888	1	0.869888	0	0	0	0	0	0	0	0	0	0	0.450402	0	0
Florida+London	1	0.869888	1	0	0	0	0	0	0	0	0	0	0	0.541547	0	0
Gemma3:12_i	0	0	0	1	1	1	1	1	1	1	1	1	1	0	1	1
Gemma3:12-QAT_i	0	0	0	1	1	1	1	1	1	1	1	1	1	0	1	1
Gemma3:27_i	0	0	0	1	1	1	1	1	1	1	1	1	1	0	1	1
Gemma3:27-QAT_i	0	0	0	1	1	1	1	1	1	1	1	1	1	0	1	1
Llama3.3:70b_i	0	0	0	1	1	1	1	1	1	1	1	1	1	0	1	1
Llama4:16x17b_i	0	0	0	1	1	1	1	1	1	1	1	1	1	0	1	1
Gemma3:12_c	0	0	0	1	1	1	1	1	1	1	1	1	1	0	1	1
Gemma3:12-QAT_c	0	0	0	1	1	1	1	1	1	1	1	1	1	0	1	1
Gemma3:27_c	0	0	0	1	1	1	1	1	1	1	1	1	1	0	1	1
Gemma3:27-QAT_c	0.541547	0.450402	0.541547	0	0	0	0	0	0	0	0	0	0	1	0	0
Llama3.3:70b_c	0	0	0	1	1	1	1	1	1	1	1	1	1	0	1	1
Llama4:16x17b_c	0	0	0	1	1	1	1	1	1	1	1	1	1	0	1	1

Note: Computed pairwise for each imagination network. The above matrix is symmetrical across the diagonal. The postfixes “_i” and “_c” to LLM models denote LLM-Independent and LLM-Cumulative tasks, respectively.